Dynamical intermediates in the collapse of semiflexible polymers in poor solvents

B. Schnurr[1], F. C. MacKintosh[1] and D. R. M. Williams[2,3]

[1] *Department of Physics & Biophysics Research Division, University of Michigan Ann Arbor, MI 48109-1120, USA*
[2] *Institute of Advanced Studies, Research School of Physical Sciences and Engineering The Australian National University - Canberra, ACT 0200, Australia*
[3] *School of Chemistry, University of Sydney - NSW 2006, Australia*

Abstract. – We investigate, by a Brownian Dynamics (BD) simulation, the collapse of a single, semiflexible or stiff polymer in solution, in the presence of short-range, attractive interactions. In contrast to the mechanism for flexible chains, our results suggest that the collapse occurs via a series of long-lived, metastable intermediates. These intermediates form a well-defined, hierarchical family of conformations. Experiments with DNA condensation have shown similar shapes, which were described as "tennis racquets". In addition to our primary observation concerning the collapse pathways of stiff filaments, we note that, in the absence of fluctuations (upon annealing), the shape of these intermediates can be calculated exactly in certain limits, and is given by a particular case of Euler's elastica. This shape is unique up to an overall scale factor determined by the parameters for bending stiffness and short-range attraction.

One of the most basic properties of an isolated polymer chain is its size and shape under various solvent conditions [1–3]. For completely flexible chains in good solvent the monomers effectively repel one another, favoring contact with the solvent, and a swollen coil is formed. In poor solvent the monomers attract one another, and an isolated chain forms a compact globule, roughly spherical in shape, which minimizes the surface area between monomers and solvent. However, in contrast to the flexible case, many polymers exhibit substantial bending stiffness, which makes a compact globule unfavorable because it involves a large amount of bending. Such chains are described by the worm-like chain model [3], and examples include many biopolymers such as F-actin and DNA as well as some synthetic polymers such as kevlar. Semiflexible polymers thus introduce a new balance to this collapse: bending stiffness, favoring extended conformations, competes with the effective self-affinity of a filament in poor solvent, which favors compact structures with maximal overlap.

Questions of equilibrium statistical mechanics often have simple answers which can be found at least qualitatively by intuition. The same cannot be said for questions involving

dynamics. For instance, a sausage model was first proposed for the collapse of a flexible polymer [4]. The actual dynamics were recently found by computer simulation which showed that the collapse proceeds instead by the formation of a pearl necklace and the gradual diffusion of large pearls from the chain ends [5]. Our system of interest here is a semiflexible or stiff chain, and its collapse dynamics upon quenching in poor solvent could be expected to have similarly interesting features.

It is known from experiments [6–11] and Monte Carlo simulations [12,13] that semiflexible chains can form toroids, which reduce the monomer-solvent contacts without incurring as much bending penalty as a sphere or globule. Although there is no theoretical proof that a torus is the ground state, there is clear experimental evidence for its formation and stability, and its detailed features and packing have received considerable theoretical attention [9,10,14,15]. In this letter, we present a different aspect of this phenomenon: to study the actual time evolution of filament collapse, which Monte Carlo cannot address, we chose a molecular dynamics (Brownian dynamics) simulation and found not only additional evidence for the stability of the torus, but also, and more importantly, interesting aspects to the kinetic collapse process. We emphasize that we do not describe a system in equilibrium and therefore cannot discuss our results in the language of phase transitions. The analog of the coil-globule transition for semiflexible chains is addressed elsewhere with more appropriate techniques for that question, in refs. such as [12,16]. Rather, we study the kinetic pathways of collapse of an individual chain at constant temperature upon a quench in effective solvent quality. Given an extended chain with bending stiffness, we ask: what are the pathways of collapse towards a ground state, and can we confirm this ground state to be the torus?

Simulation details. –   Our simulation applies a standard Brownian dynamics (BD) algorithm [2] to a bead-and-spring model of the polymer chain. In order to capture the most general features of this process, we chose this most basic model, which does not include any of the biological machinery or structural details involved in a real problem such as DNA condensation. For a polymer chain in solution, with length scales at the molecular level, all motions are overdamped (at low Reynolds numbers), making BD an efficient dynamical tool. For simplicity, our simulation is two-dimensional—the chain moves only in the plane. To allow for filament crossing, we omit any chain-chain exclusion so that the chain can intersect itself freely. Consequently, the effects of topological entanglements are neglected. Our simulation also omits hydrodynamic interactions between particles, which would likely give corrections to time scales and such, but not change our findings concerning kinetic pathways and intermediate states.

Experimentally, this setup could be realized by a biopolymer chain constrained to two dimensions by its affinity to a charged lipid bilayer [17], a mica surface [8,18], or a treated microscope cover slip [19].

Our dynamics are based on a Langevin equation of the form [2]

$$\xi \frac{\mathrm{d}x_i}{\mathrm{d}t} = -\frac{\partial U}{\partial x_i} + \eta_i(t) = F_{x_i} \tag{1}$$

for each bead i, where ξ is the coefficient of viscous drag ($\boldsymbol{F}_{\mathrm{visc}} = \xi\boldsymbol{v}$) and η is the random noise. In the BD simulation, each bead is displaced by $\Delta x_i = (F_{x_i}/\xi)\Delta t$ in each time step Δt. The potential U contains all interactions internal to the chain,

$$U = U_{\mathrm{bend}} + U_{\mathrm{solvent}} + U_{\mathrm{spring}}, \tag{2}$$

where U_{bend} represents the bending energy, U_{solvent} is a short-range attraction between beads (mimicking poor solvent conditions) that induces collapse, and U_{spring} includes a very stiff lon-

gitudinal compliance for each bead-bead link along the chain. The electrostatics of counterion-induced attraction in polyelectrolytes is described in [20] and references therein.

U_{bend} is implemented as a discrete analog of the worm-like chain [2,3]:

$$U_{\text{bend}} = \frac{\kappa}{2b} \sum_i \theta_i^2, \tag{3}$$

where the $\{\theta_i\}$ are the bond angles, b is the equilibrium link length, and κ is the bending modulus. The persistence length of such a chain in two dimensions is $\ell_{\text{p}} = 2\kappa/k_{\text{B}}T$. For the parameters used here, a persistence length consists of 15 links. For the attractive interaction U_{solvent} we chose a pairwise quadratic potential between beads with a finite-range cutoff of $10/3$ link lengths and a depth of $5/8\ k_{\text{B}}T$. The last term, U_{spring}, models the links between beads as quadratic springs with equilibrium length b. Their force constant exceeds that of the poor solvent interaction by a factor of 200 which allows for deviations from the equilibrium link length b of about 30% due to the thermal fluctuations at $k_{\text{B}}T$. This represents a compromise between stiffer springs modeling a more realistically inextensible chain and weaker springs allowing for longer simulation time steps without interfering with the spring relaxation time. Every chain was initialized with a Gaussian distribution of bond angles and then allowed to thermalize in the absence of contact interactions over several times the longest relaxation time of the filament. Attractive interactions were switched on suddenly (solvent quality quenched) at $t = 0$.

We have not investigated to what degree the dynamical results depend on our choices of parameters. Any modeling of a particular system would need to include the various molecular details we have ignored here. Because of the relatively long run time required for each simulation, it appeared impractical to systematically map out the phase space of all parameters. Instead we reasonably approximated the effective physical conditions in experiments which observe such an induced collapse. The filament length L for the majority of runs were about $7\ell_{\text{p}}$, long enough to make contacts through thermal motion alone likely.

Dynamics results. – The left panel in fig. 1 shows nine snapshots taken during the typical dynamical evolution of a relatively short chain (50-mer, about $3\ell_{\text{p}}$). The sequence shows a progression through well-defined stages, identified by four types of chain conformations: extended chain (A-B), single-headed racquet (D-E), higher-order or multiple-headed racquets (F-G), and finally the torus (H-I). The right panel in fig. 1 shows, for the same run, the end-to-end distance $R_{\text{e-e}}$ of the filament as a function of time. Distinct changes in $R_{\text{e-e}}$ correlate well with conformational transitions: *e.g.*, the rapid drop in the vicinity of C and D corresponds to the equalization of length between the two arms of a newly formed racquet. It is important to note that the described conformations persist in time, as seen by the quasi-plateaus in the right panel of fig. 1, each lasting for the considerable time of $\sim 10^6$ BD steps. These persistent structures are seen throughout most of our BD runs, suggesting that metastable intermediates are a general feature in this collapse. Structures similar in appearance to the racquet configuration have previously been observed (and named "tennis racquets") in electron microscopy of DNA during condensation [7].

Over one hundred runs follow the theme of fig. 1, with variations in the exact sequence of structures and the degree of completion. This particular example was chosen as it displayed most of the observed features in a single run. Some sequences skip various of these intermediates: *e.g.*, an extended chain can roll up into a torus from the ends directly. However, it appears from all our observations so far that transitions between configurations occur only in the direction (in time) shown in the sequence of snapshots, although not every run reaches completion in the torus. This directionality suggests that the progression is energetically
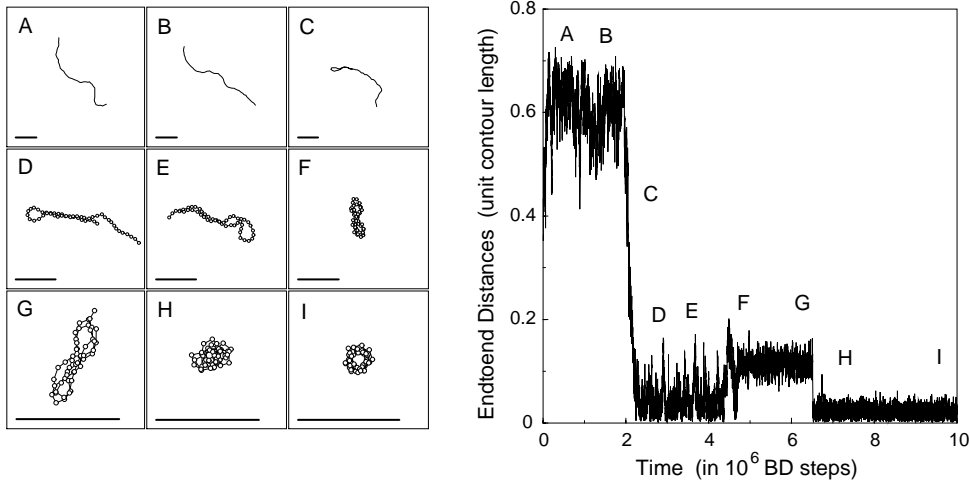
Fig. 1 – Left panel: Time evolution snapshots A-I of a single chain (50-mer, about $3\ell_{\mathrm{p}}$) during a simulation of 10^7 BD steps. We see the chain go through the stages: extended chain, single racquet, multiple racquets, and torus. The scale bars are an arbitrary unit length and merely indicate the increasing degree of magnification. Right panel: End-to-end distances $R_{\mathrm{e\text{-}e}}$ *vs.* time, for the same run. The letters indicate the correspondence to the various conformational states shown on the left. As the structures get more compact, the variance in $R_{\mathrm{e\text{-}e}}$ is increasingly supressed.

driven, with the torus representing the presumed ground state, and that large energy barriers between the intermediates are responsible for their metastability [21].

Our general picture is thus as follows: after quenching the solvent, the chain typically fluctuates randomly until a loop forms from one end (fig. 1C). We distinguish two cases: if two segments of the chain first meet at a tangent angle of 2π, the loop immediately rolls up into a torus. More commonly, as it requires less bend in the filament overall, segments meet at an angle π and form a racquet head, whose two arms rapidly equalize in length (fig. 1C through E) and form a neck region. This process is driven by an increasing number of monomer-monomer contacts without increase in bending penalty. The resultant structure is the first in a hierarchy of possible long-lived intermediates. A next step may involve forming another head at the neck end of such a racquet. By a series of similar events, higher-order racquets (such as in fig. 1F and G) are produced, making up a family of metastable intermediates [21]. In this case, formation of the torus occurred by separation of the filaments in the neck by random fluctuations. However, good statistics on this step would require much longer run times.

Figure 2 shows the number of chains per conformation among over one hundred chains as a function of time. The number in each species initially increases. If a torus were the ground state, one would expect all other species to vanish over time, while the torus population should grow and finally saturate. We infer that our runs are not long enough to show this full evolution, but merely its early stages. In fact, the data in fig. 2 suggest that only about 10% of our chains actually became toroids during the time allowed. The majority of filaments were trapped in the local minimum of one of the racquet states. However, we take it as evidence for the stability of the torus that no transitions were observed from a torus to either racquets or open filaments. To date, long processing times have prevented us from gathering better statistics on longer runs. Each run in fig. 2 takes about a day on a dual-processor Pentium CPU.
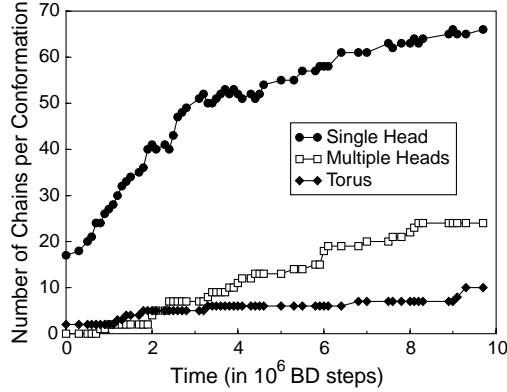
Fig. 2 – Statistics of chain conformations (100-mer) with time for a given set of parameters. The non-zero initial values result from the onset of compact structures immediately following thermalization and the change in solvent quality. Longer runs than these should reveal the late-stage behavior, where we expect all racquets to vanish in favor of toroids.

Analytical racquet shape. – Having identified the racquet head as the common element in the intermediate states, we calculate its geometrical shape (see fig. 3) in the absence of thermal fluctuations. The general problem of the bending of a thin rod by forces and couples applied at its ends only is known as the *elastica*. Its solutions were first studied by Euler in 1744. The particular solution we seek is schematically drawn in fig. 51 of ref. [22].

Since the problem is symmetric about the neck axis, we consider one half of the head only, and label its contour length by L. Starting at the curved end, the tangent angle increases from $\theta = 0$ at arc length $s = 0$ to $\theta = \pi/2$ at $s = L$ (where the head joins the handle). As a constraint, this curve must be traced out through a length L and with zero net displacement in the direction perpendicular to the axis of symmetry: $\int_0^L \mathrm{d}s \, \cos\theta(s) = 0$. The elastica is solved by minimizing the bending energy $U = \frac{\kappa}{2} \int_0^L \mathrm{d}s \, (\mathrm{d}\theta/\mathrm{d}s)^2$ subject to the constraint. This leads to the differential equation

$$\frac{\mathrm{d}^2\theta}{\mathrm{d}s^2} = -\omega^2 \sin\theta(s) \,, \tag{4}$$

where ω^2 is a Lagrange multiplier. Equation (4) also describes a simple pendulum undergoing large oscillations, with arc length corresponding to time. It has the solution $\theta(s) = 2\sin^{-1}[k\,\mathrm{sn}(\omega s)]$ and a period $T = 4K(k)/\omega$, where $K(k)$ and $\mathrm{sn}(\omega s)$ are elliptic functions. Our goal is to find the two unknown parameters, k and ω. These can be found by calculating the time (or arc length) required to go from $\theta = 0$ through $\pi/2$ to $\theta = \theta_m$ and back to $\theta = \pi/2$. Here, θ_m is the amplitude of the pendulum. Equating this time to L gives one equation,

$$\omega L = K(k) + F\left[k, \sin^{-1}\left(\frac{1}{k\sqrt{2}}\right)\right] \,. \tag{5}$$

A second equation comes from the constraint, which yields $L - 2k^2[I(0, T/4) + I(T/4, L)] = 0$, where $I(x, y) \equiv \int_x^y \mathrm{d}s \, \mathrm{sn}^2(\omega s)$. Solving numerically gives $k = 0.85509$ and $\omega L = 3.22383$. The solution thus corresponds to a pendulum with an amplitude $\theta_m = 2\sin^{-1}(k) = 2.05146$ radians. Plotting both (symmetric) halves of this particular elastica results in a curve indistinguishable from the one in fig. 3 showing a simulated chain upon annealing. The racquet
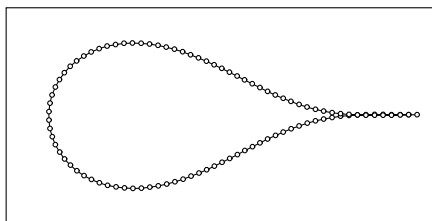
Fig. 3 – Annealed racquet from the numerical simulation. Once formed, the "temperature" was slowly reduced to yield the annealed shape for comparison with the formal solution from elasticity theory. The curves superpose to within the linewidth.

shape is unique up to an overall scale factor; it is the same for macroscopic "thin rods" as well as microscopic polymer chains (when annealed), provided there are no long-range interactions.

Discussion. – There is a large literature on the collapse of *flexible* chains [5]. The collapse of single, *stiff* chains has also been studied previously, using Monte Carlo simulations [12, 13, 16], but was approached primarily as a phase transition. Reference [12] describes structures which appear similar to our single racquets, but differ in conformational detail and interpretation. In contrast and as a complementary technique to molecular dynamics, Monte Carlo simulations do not provide actual time evolution and can thus not describe the dynamical formation of intermediates and their persistence in time. Only one of the above references [13] discusses Langevin dynamics of stiff chains in addition to Monte Carlo simulations, but does not report any metastable intermediates.

Biopolymers have increasingly provided convenient experimental systems with the large persistence lengths needed for the visualization of single molecules with optical techniques. In preliminary experiments [19], fluorescently labeled filaments of F-actin in multivalent salt buffers have formed rings and single-headed racquets with features on the micron scale. Somewhat different conformations—flower-shaped intermediates— have been observed by AFM in the condensation of DNA on mica [18].

We have shown that single, semiflexible chains with short-range attractive interactions (in poor solvent) evolve toward a compact state (a torus, the presumed ground state) via a series of long-lived, intermediate states. These intermediates appear to be metastable, due to large bending energy barriers. Certain limitations in our study are, first of all, that the simulation considers chain motion only in the plane, although we do allow for self-intersections. Secondly, we have considered only relatively short chains. Preliminary examples of longer chains (up to $20\ell_{\mathrm{p}}$) intermittently displayed a superstructure of racquets within racquets, before turning into a multiple racquet with long neck acting as a renormalized, stiffer filament that finally collapsed to a torus. Finally, we note that our results for the collapse of a stiff polymer chain differ qualitatively from those available for flexible polymers [5]. The collapse of a flexible chain proceeds without long-lived intermediates, whereas a persistent chain appears to spend a large amount of time in non-trivial metastable states.

* * *

REFERENCES

[1] de Gennes P. G., *Scaling Concepts in Polymer Physics* (Cornell University Press, New York) 1979.
[2] Doi M. and Edwards S. F., *The Theory of Polymer Dynamics* (Clarendon Press, Oxford) 1988.
[3] Grosberg A. Yu. and Khokhlov A. R., *Statistical Physics of Macromolecules* (AIP Press, New York) 1994.
[4] de Gennes P. G., *J. Phys. (Paris) Lett.*, **46** (1985) L639.
[5] Ostrovsky B. and Bar-Yam Y., *Europhys. Lett.*, **25** (1994) 409; Chu B., Ying Q. C. and Grosberg A. Yu., *Macromolecules*, **28** (1995) 180; Buguin A., Brochart-Wyart F. and de Gennes P. G., *C. R. Acad. Sci. Paris, Ser. II*, **322** (1996) 741; Dawson K. A., Timoshenko E. G. and Kuznetsov Y. A., *Physica A*, **236** (1997) 58; Halperin A. and Goldbart P. M., *Phys. Rev. E*, **61** (2000) 565.
[6] Bloomfield V. A., *Biopolymers*, **44** (1997) 269.
[7] Li A. Z., Fan T. Y. and Ding M., *Science in China Series B*, **35** (1992) 169.
[8] Fang Y. and Hoh J. H., *Nucl. Acids Res.*, **26** (1998) 588; Fang Y., Spisz T. S. and Hoh J. H., *Nucl. Acids Res.*, **27** (1999) 1943.
[9] Hud N. V., Downing K. H. and Balhorn R., *Proc. Natl. Acad. Sci. USA*, **92** (1995) 3581; Hud N. V., *Biophys. J.*, **69** (1995) 1355.
[10] Vasilevskaya V. V. *et al.*, *Biopolymers*, **41** (1997) 51.
[11] Yoshikawa Y., Yoshikawa K. and Kanbe T., *Biophys. Chem.*, **61** (1996) 93.
[12] Noguchi H. *et al.*, *Chem. Phys. Lett.*, **261** (1996) 527; Noguchi H. and Yoshikawa K., *Chem. Phys. Lett.*, **278** (1997) 184; Noguchi H. and Yoshikawa K., *J. Chem. Phys.*, **109** (1998) 5070.
[13] Byrne A., Timoshenko E. G. and Dawson K. A., *Nuovo Cimento D*, **20** (1998) 2289.
[14] Bright J. N. and Williams D. R. M., *Europhys. Lett.*, **45** (1999) 321.
[15] Grosberg A. Yu., *Biofizika*, **24** (1979) 32; Ubbink J. and Odijk T., *Biophys. J.*, **68** (1995) 54; Ubbink J. and Odijk T., *Europhys. Lett.*, **33** (1996) 353; Park S. Y., Harries D. and Gelbart W. M., *Biophys. J.*, **75** (1998) 714; Golo V. L., Kats E. I. and Yevdokimov Y. M., *J. Biomol. Struct. Dyn.*, **15** (1998) 757.
[16] Doye J. P. K., Sear R. P. and Frenkel D., *J. Chem. Phys.*, **108** (1998) 2134.
[17] Maier B. and Rädler J. O., *Phys. Rev. Lett.*, **82** (1999) 1911.
[18] Fang Y. and Hoh J. H., *J. Am. Chem. Soc.*, **120** (1998) 8903.
[19] Janmey P. A. *et al.*, personal communications; Schnurr B., Möhler W. and Schmidt C. F., unpublished results.
[20] Grønbech-Jensen N. *et al.*, *Phys. Rev. Lett.*, **78** (1997) 2477; Hansen P. L., Svenšek D., Parsegian V. A. and Podgornik R., *Phys. Rev. E*, **60** (1999) 1956.
[21] Schnurr B. *et al.*, in preparation.
[22] Love A. E. H., *A Treatise on the Mathematical Theory of Elasticity* (Dover Publications, New York) 1944.